Supplementary Data

Effect of Freezing Conditions on Distances and Their Distributions Derived from Double Electron Electron Resonance (DEER): A Study of Doubly-Spin-Labeled T4 Lysozyme

Elka R. Georgieva[†], Aritro S. Roy[†], Vladimir M. Grigoryants[‡], Petr P. Borbat[†], Keith A. Earle[#,†], Charles P. Scholes[‡], and Jack H. Freed[†] *

[†]Department of Chemistry and Chemical Biology and ACERT, Cornell University, Ithaca, NY 14853

[‡] Department of Chemistry, University at Albany, 1400 Washington Avenue, Albany, NY 12222

[#]Department of Physics, University at Albany, 1400 Washington Avenue, Albany, NY 12222

Data analysis and absolute distance error

All distance distributions were extracted from experimentally obtained DEER time-domain data. First, the base line (background signal from inter-molecular spin-spin interactions) in the time-domain was defined as the best linear fit on a log scale and then it was subtracted from the raw DEER time-domain signal. The remaining signal, which reflects the dipole-dipole interaction between coupled electron spins of interest, was normalized in the original scale of spin-echo amplitude units based on the assumption that at zero evolution time the signal starts from unity. Thereafter, the distances and distance distributions were reconstructed by using the Tikhonov

Regularization Method [S1] and refined by the Method of Maximum Entropy (MEM), version with no additional base-line optimization [S2]. To estimate the error in reconstructed distances due to uncertainties in defining the background signal in time-domain data, we performed an additional adjustment of our already background-corrected DEER signals by using the version of MEM for non-linear base-line optimization [S2]. Then we compared the profiles of distance distributions obtained by using the versions of MEM without and with base-line optimization. We found negligible differences in the positions of the maximal distances as well as distance distributions. Therefore we consider the error in the obtained distance distributions to be negligible within the sensitivity of the distance reconstruction algorithm used.

We used a home written program to construct time-domain signals from the reconstructed distance distributions. The simulated time-domain signals are virtually indistinguishable from those obtained experimentally.

The procedure for data processing and analysis is demonstrated in Figure S1 with four examples: (i) doubly spin-labeled with MTSL mutant 8C/128C; (ii) doubly spin-labeled with 4-Bromo MTSL mutant 8C/128C; (iii) doubly spin-labeled with MTSL mutant 65C/135C; and (iv) doubly spin-labeled with 4-Bromo MTSL mutant 65C/135C.

(i) Doubly spin-labeled with MTSL mutant 8C/128C

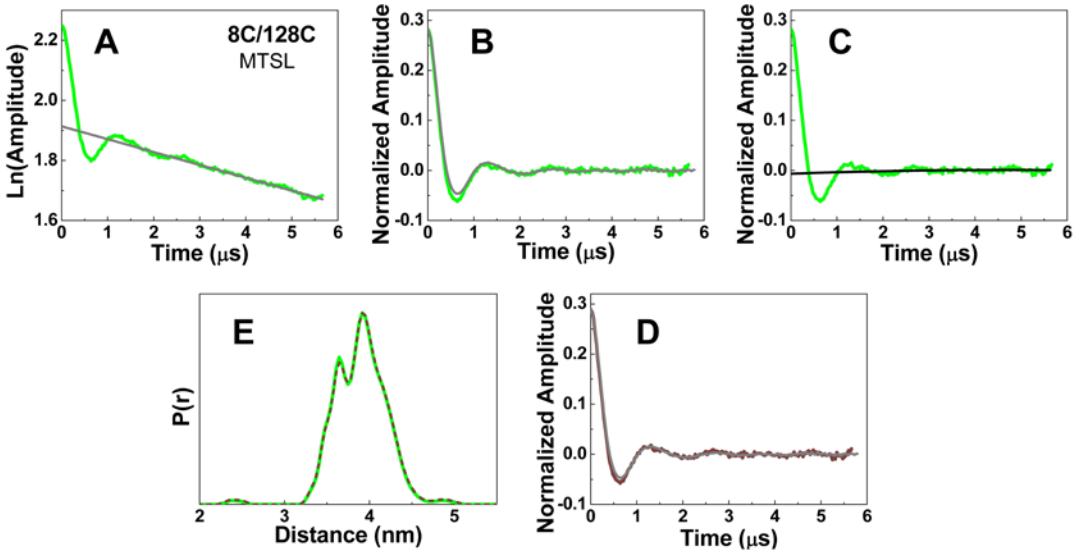

(ii) Doubly spin-labeled with 4-Bromo MTSL mutant 8C/128C

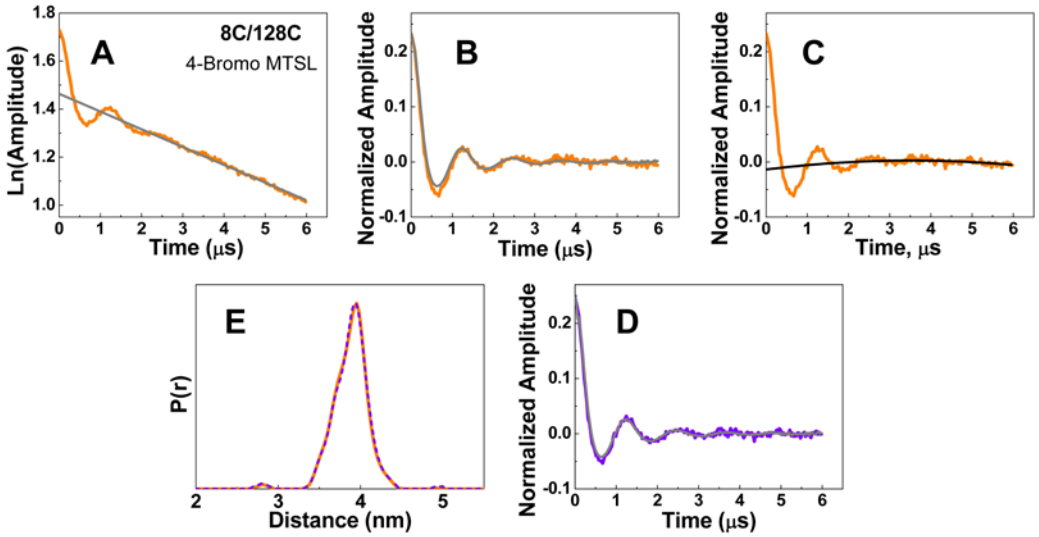

Figure S1. Continues on the next page

(iii) Doubly spin-labeled with MTSL mutant 65C/135C

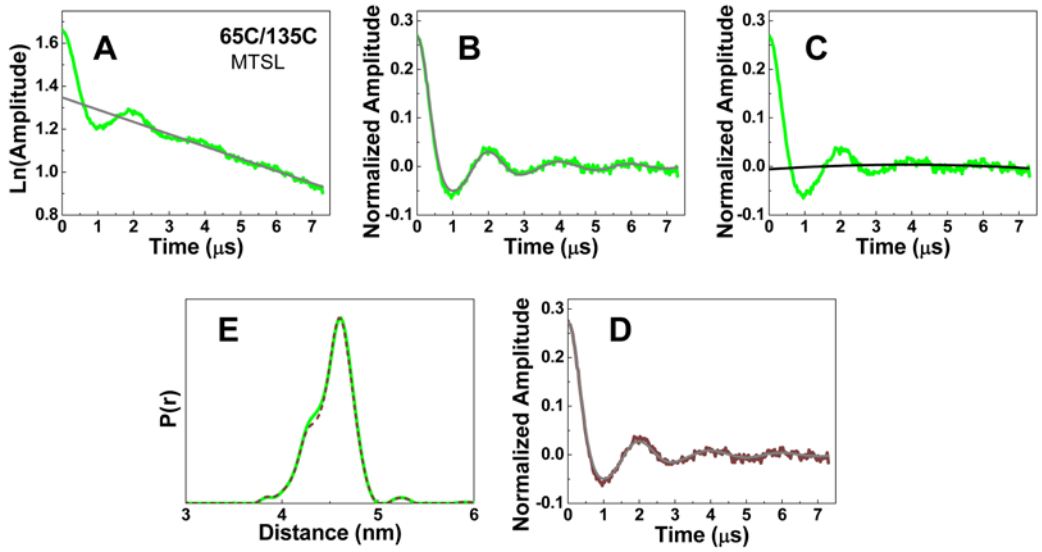

(iv) Doubly spin-labeled with 4-Bromo MTSL mutant 65C/135C

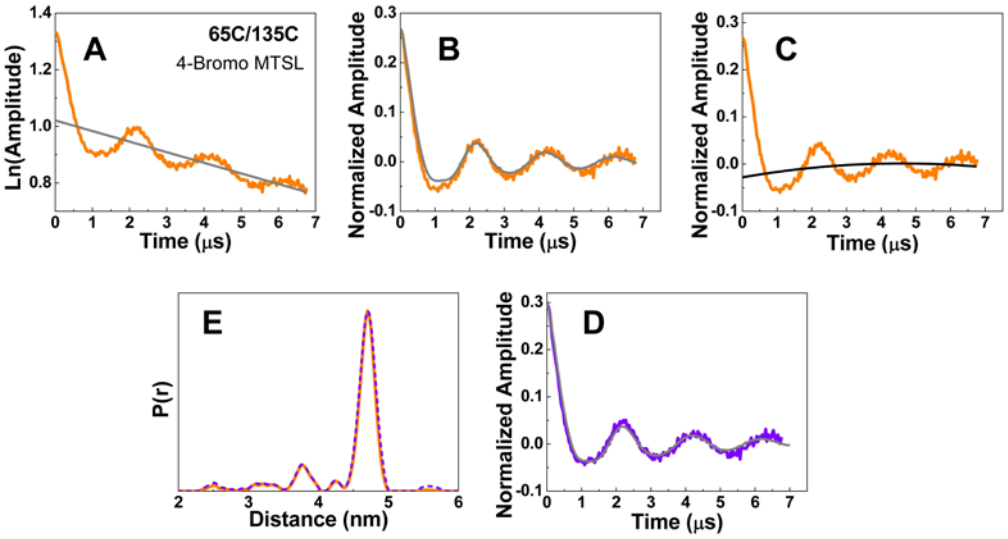

Figure S1. The procedure for DEER data processing and analysis is demonstrated for mutants 8C/128C and 65C/135C spin-labeled with either regular MTSL or 4-Bromo MTSL:

Panel A shows the raw DEER signals on a log scale (either in green for MTSL or orange for 4-Bromo MTSL) and the background approximation by a linear base-line (gray);

Panel B shows the base-line subtracted and normalized time-domain data, which are compared with the simulated time-domain data after distance reconstruction by using Tikhonov regularization method [S1] and MEM with no additional base-line optimization [S2].

Panel C shows the additional base-line adjustment of the already background corrected and normalized DEER signal by the version of MEM for non-linear background optimization [S2]. The additional base-line is plotted in black.

Panel D shows the adjusted DEER signal (in brown for MTSL and purple for 4-Bromo MTSL) after the subtraction of the additional base-line (in black in panel C). This signal is compared with the simulated time-domain signal after distance reconstruction by using Tikhonov regularization method and MEM with non-linear base-line optimization.

Panel E compares the distance distributions reconstructed by Tikhonov regularization method and refined by MEM without (solid lines in green or orange) or with base-line optimization (dashed lines in brown or purple).

The samples were regularly shock-frozen in liquid N_2 and contain 30 % Glycerol.

Probing the protein conformation vs spin-label rotamer conformation: Analysis of possible spin-label rotamers

To study the origin of complex distance distributions obtained for doubly spin-labeled with MTSL T4L mutants, we performed an analysis by using molecular modeling software (MMM) [S4] which predicts possible distributions of rotamers of MTSL, and consequently distance

distributions, based on force fields and existing structures at atomic resolution. We pre-calculated the possible rotamers and resulting distance distributions at an ambient temperature of 298K and at 175K. The former was expected to be close to our distance distribution for rapidly-frozen samples, based on the assumption that high (room)-temperature conformers are trapped; the latter is expected to be closer to the distributions for slowly frozen samples in liquid N_2.

A large number of T4L structures at atomic resolution exist [S5-S8]. However, for our analysis we selected four featured structures of T4L: WT T4L, PDB code 3LZM [S5], which represent the protein in closed conformation; T4L in open conformation stabilized by the M6I mutation, PDB code 150Lc [S6]; L99A T4L, PDB code 3DMV, which mutant is able to bind hydrophobic ligands and has a virtually indistinguishable crystal structure from those of the WT enzyme [S7]; and a recent solution structure of L99A T4L revealed by NMR and assigned to a transient exited state of this mutant with a life-time of about 1 ms, PDB code 2LCB [S8]. Interestingly, the authors of this NMR study [S8] proposed that the observed co-existence of ground and exited states of L99A T4L, represented by different structures, is related to the function. Further, they projected this structural inter-conversion on the general view for protein plasticity as a base for functionality. Given this, we aimed to understand whether any fluctuations in the protein structure happening on the time-scale of our freezing rates, could be trapped and contribute to the observed complex distance distributions.

The results of our analysis are plotted in Figure S2 together with the experimental distance distribution for all doubly spin-labeled with MTSL T4L mutants: 8C/44C, 8C/128C, 65C/128C and 65C/135C.

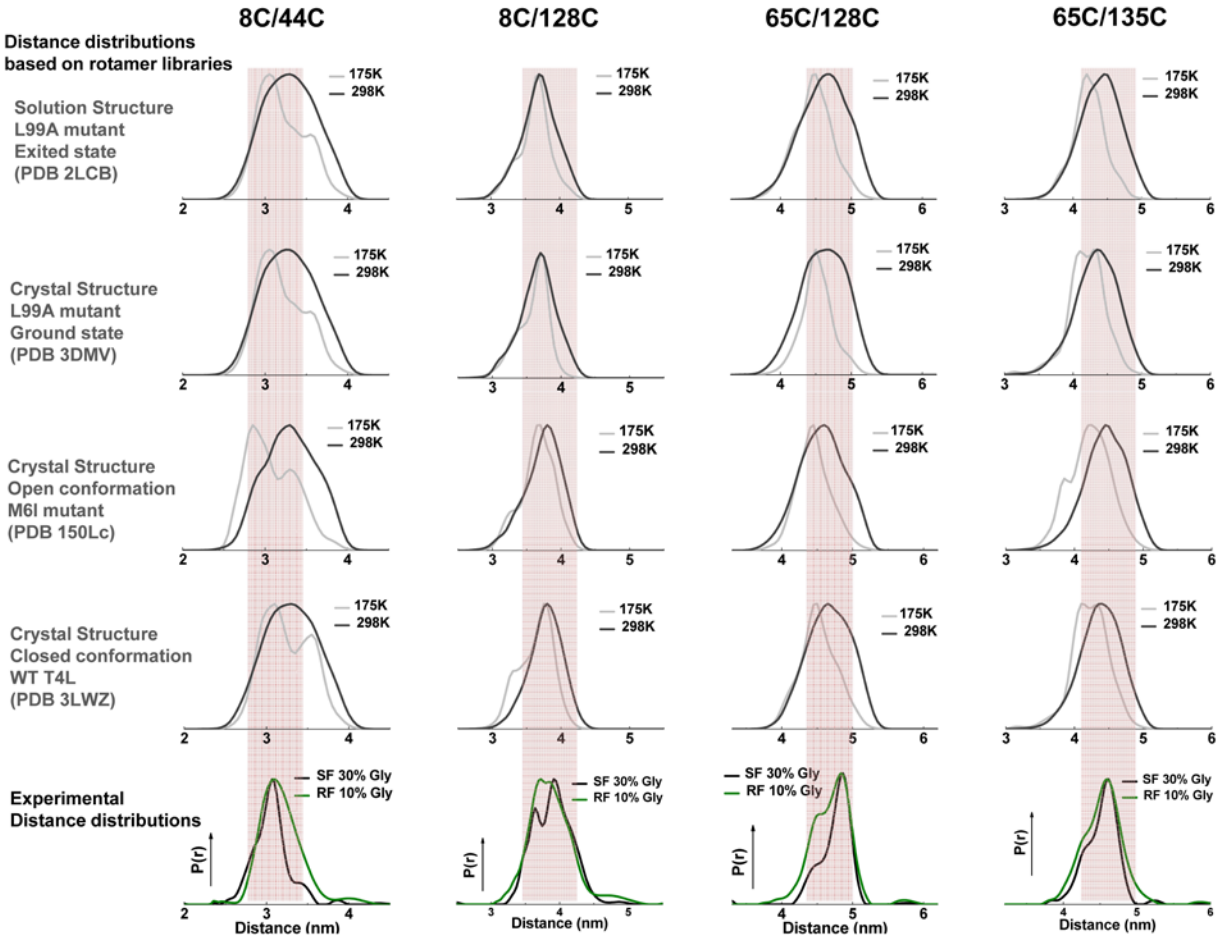

Figure S2. Pre-calculated distance distributions at 175K and 298K by using MMM [S4] based on four existing structures of T4L are compared with our experimentally obtained distance distributions based on our very high quality DEER data for all four doubly T4L cysteine mutants studied. The distance distributions are normalized in arbitrary units to unity at maximum intensity.

We found: (i) A large number of rotamers was obtained for each solvent exposed spin-labeled residue regardless of the protein structure used. The resulting distance distributions between each pair of spin-labeled residues are complex; (ii) The resolution of calculated distance distributions is insufficient to distinguish contributions from protein conformations; (iii) There is a reasonable agreement between pre-calculated distance distributions based on rotamer libraries [S4] and our experimentally obtained distance distributions. However, the distributions from experiment are generally narrower than the predicted ones, which may indicate a smaller number of actual spin-label rotamers.

Based on insufficient resolution of our experiment and also theoretical analysis, we are not able to conclude whether different protein conformers contribute to the complex distance distribution, that we obtained by DEER spectroscopy for doubly spin-labeled cysteine mutants of WT* T4L.

Doubly spin-labeled mutant 8C/128C: Testing possible orientation effects

We obtained the most intriguing distance distributions for the doubly spin-labeled T4L mutant 8C/128C when it was labeled with MTSL, where a bimodal distance distribution was observed when the protein was shock-frozen in liquid N_2. However, a significantly narrowed distance distribution was observed when T4L was labeled at the same positions with 4-Bromo MTSL (Figure 4, A, in the main text). Therefore, we have concluded that the bimodal distance distribution is a result of the presence of multiple MTSL rotamers, and some of them are not available for the Bromo-substituted MTSL due to its greater rigidity. One more possibility for the observed multi-feature distance distribution in the case of spin-labeled residues 8C/128C might be an orientation effect [S9], even though both of the residues are solvent exposed and MTSL conformers are expected to be randomly oriented.

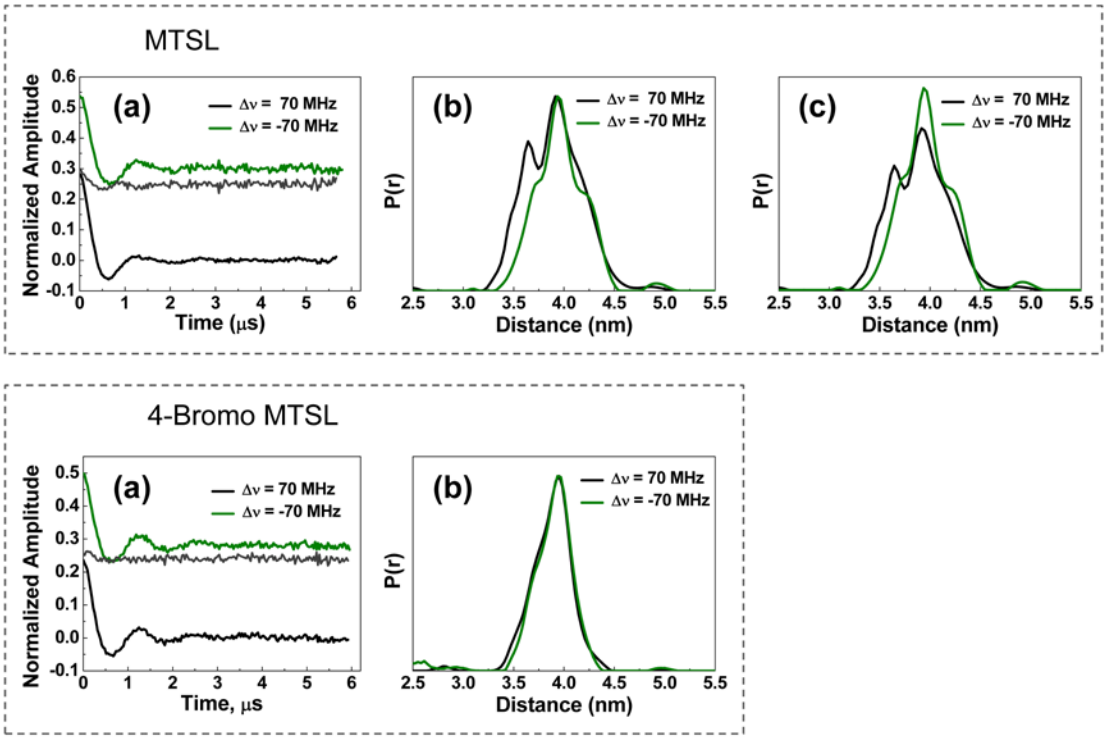

Figure S3. Experimental base-line corrected and normalized DEER signals and reconstructed distances and distance distributions for T4L mutant 8C/128C spin-labeled with MTSL (upper panel) and 4-Bromo MTSL (lower panel) at two different frequency separations between detection and pump pulses of 70 MHz (black) and -70 MHz (green): (a) The time-domain signals obtained at pulse frequency separation of 70 MHz and -70 MHz are plotted in black and green, respectively. Residuals between the DEER signals obtained at 70 MHz and -70 MHz are plotted in gray; (b) Reconstructed distances and distance distributions are plotted after normalizing their intensities to unity in arbitrary units; (c) Normalized to unity distances and distance distributions are plotted.

To test this possibility we used both the samples spin-labeled with MTSL and 4-Bromo MTSL of mutant 8C/128C and recorded DEER traces at a separation of 70 MHz between frequencies of detection and pump pulses, and also a separation of -70 MHz. This was achieved by changing the position (frequency) of the detection pulses, whereas the frequency of the pump pulse was not changed and positioned at the center of the nitroxide spin-label spectrum at 17.3 GHz. Time domain DEER signals and reconstructed distances distributions are plotted in Figure S4.

Differences attributed to spin-label orientation were observed when regular MTSL was used. However, the DEER traces and reconstructed distance distributions for protein spin-labeled with 4-Bromo MTSL were very similar for both frequency separations of 70 MHz and -70 MHz between detection and pump pulses. We believe that, in the case of MTSL only some of the rotamers with appropriate orientation relative to the inter-spin vector contribute significantly to the angular dependence [S10], and these rotamers are not populated when protein is labeled with 4-Bromo MTSL.

References

[S1] Y.W. Chiang, P.P. Borbat, J.H. Freed, The determination of pair distance distributions by pulsed ESR using Tikhonov regularization, J Magn Reson, 172 (2005) 279-295.

[S2] Y.W. Chiang, P.P. Borbat, J.H. Freed, Maximum entropy: a complement to Tikhonov regularization for determination of pair distance distributions by pulsed ESR, J Magn Reson, 177 (2005) 184-196.

[S3] C. Altenbach, K.J. Oh, R.J. Trabanino, K. Hideg, W.L. Hubbell, Estimation of inter-residue distances in spin labeled proteins at physiological temperatures: experimental strategies and practical limitations, Biochemistry, 40 (2001) 15471-15482.

[S4] Y. Polyhach, E. Bordignon, G. Jeschke, Rotamer libraries of spin labelled cysteines for protein studies, Phys Chem Chem Phys, 13 (2011) 2356-2366.

[S5] M. Matsumura, J.A. Wozniak, S. Dao-pin, B.W. Matthews, Structural studies of mutants of T4 lysozyme that alter hydrophobic stabilization, J Biol Chem, 264 (1989) 16059-16066.

[S6] X. Zhang, J.A. Wozniak, B.W. Matthews, Protein flexibility and adaptability seen in 25 crystal forms of T4 lysozyme, J Mol Biol, 250 (1995) 527-552.

[S7] L. Liu, W.A. Baase, B.W. Matthews, Halogenated benzenes bound within a non-polar cavity in T4 lysozyme provide examples of I···S and I···Se halogen-bonding, J Mol Biol, 385 (2009) 595-605.

[S8] G. Bouvignies, P. Vallurupalli, D.F. Hansen. B.E. Correia, O. Lange, A. Bah, R.M. Vernon, F.W. Dahlquist, D. Baker, L.E. Kay, Solution Structure of a minor and transiently formed state of a T4 lysozyme mutant, Nature, 477 (2011) 111-114.

[S9] D. Margraf, B.E. Bode, A. Marko, O. Schiemann, T.F. Prisner, Conformational flexibility of nitrixide biradicals determined by X-band PELDOR experiments, Mol Phys, 105 (2007) 2153-2160.

[S10] S.K. Misra, P.P. Borbat, J.H. Freed, Calculation of double-quantum coherence two-dimensional spectrum: Distance measurements and orientational correlations, Appl Magn Res, 36 (2009) 237-258.